Nonequilibrium Flow over a Cone

R. SEDNEY* AND N. GERBER†
Ballistic Research Laboratories, Aberdeen Proving Ground, Md.

The modifications in the flow over a cone are considered due to departure from thermodynamic equilibrium behind the shock wave. Only the effects due to vibrational relaxation are considered. The flow was calculated using the method of characteristics. The numerical technique that was successful for the cone flow involved a slight modification of the standard method. As for the case of wedge flow, there is a curved shock, a relaxation layer at the shock, and an entropy layer at the cone surface. For the cone case, the thickness of the entropy layer must vanish sufficiently far downstream from the tip. The pressure on the cone surface shows an overexpansion.

Nomenclature

C = constant appearing in temperature variation of τ
C_{pa} = frozen specific heat at constant pressure
E_i = vibrational energy
h_t = constant total enthalpy
M = Mach number
n = coordinate normal to cone surface
p = pressure
q = velocity
R = gas constant per unit mass
S = entropy
r = radial polar coordinate
s = arc length along streamlines
T = temperature
x = coordinate in freestream direction
y = coordinate normal to freestream direction
β = angle between shock and x axis
γ_a = ratio of frozen specific heats
θ = flow direction relative to x axis
Θ_i = characteristic vibrational temperature
μ = frozen Mach angle
τ = relaxation time
ξ = arc length along right characteristic
η = arc length along left characteristic
σ = arc length along shock wave
ϕ = angular polar coordinate

Subscripts

c = cone surface
w = shock wave
∞ = freestream

1. Introduction

THIS work is a continuation of our studies on the applicability of the method of characteristics to computing nonequilibrium flows. The previous work[1] considered flows over wedges and other simple two-dimensional shapes. These shapes had sharp noses, which obviated the difficulties associated with flow over blunt noses. Here the flow over a cone is discussed. The reasons for studying such simple body shapes are 1) they allow one to gain some insight into the physics of the flow and the possible numerical pitfalls of the characteristics method; and 2) it is of basic interest to see how these simple, classical, supersonic flows are modified due to departure from thermodynamic equilibrium. At the present time there even appears to be engineering interest in the high-temperature aspects of flows over wedges and cones; however, the temperature in the flows to be considered here is such that only vibrational effects are important.

It is worthwhile to give a cursory review of the other methods of analyzing nonequilibrium flows. There is the inverse method, which has so far been applied only to blunt-body flows.[2, 3] Its success is a little difficult to evaluate. It should be noted that rather stringent requirements on accuracy should be imposed here, since, for many purposes, the final results are to be used as initial data for a characteristics solution in the supersonic region, and errors in the initial data inevitably propagate and usually amplify.

Several investigators have solved flow problems by linearization of the equations with respect to freestream conditions (see the review paper by Li[4]). These solutions are interesting in their own right, but their limitations are severe due to the linearization.‡

A method that seems feasible for investigating portions of the flow is to expand in a series about frozen or equilibrium conditions.[5, 6] However, this is valid only for near frozen flow. The results given by Sedney[5] for flow over a wedge and by Napolitano[6] for flow around a corner are incorrect for near-equilibrium flow. The conditions near equilibrium must depend on the previous flow history, which is not taken into account in such an expansion.[1]

The streamtube method,[7, 8] where it is necessary to assume a pressure distribution, has been used for the flow along the body and also within the shock layer. The accuracy of this method has not been assessed yet.

Another method that seems promising but has not been tested extensively involves the application of the Dorodnitsyn integral technique to nonequilibrium flow.[9]

As for previous work using characteristics, Cleaver[10] computed the flow around a corner for a Lighthill ideal dissociating gas. Three cases were studied for small turning angles, which makes it difficult to say if the method is accurate enough for the cases in which large changes occur in the flow. For the same model of gas, Capiaux[11] computed flows over a wedge. The numerical method seems to be the standard one, but the coordinates are (ψ,y), where $\psi(x,y)$ is the stream function, and x and y are Cartesian coordinates. The author states that the accuracy is increased by using these coordinates. However, the results given appear to be wrong, since the known asymptotic values of shock angle and surface pressures are not attained.§

Presented at the IAS 31st Annual Meeting, New York, January 20–23, 1963; revision received August 20, 1963. The authors wish to express their appreciation to Donald Taylor, who programmed the computations for the BRLESC, and also to Ray Makino and Joan M. Bartos.

* Research Physical Scientist, Exterior Ballistics Laboratory.
† Research Aerospace Engineer, Exterior Ballistics Laboratory.

‡ Lee[15] has analyzed nonequilibrium flow over a wedge by applying a linear perturbation to uniform frozen flow behind a shock wave. The limitations are not as severe for this approach, e.g., large wedge angles can be allowed. This analysis yields formulas for the flow variables and shock wave shape which agree, but only qualitatively, with results in Ref. 1.

§ In the revised version of this work,[16] the results were changed so that the correct asymptotic values were attained.

This illustrates the fact[1] that the validity of the results of a characteristics computation for nonequilibrium flow depends on the numerical technique used and/or on the choice of dependent variables. These are much less critical for equilibrium or frozen flow computations. In our previous work,[1] two numerical techniques were used, one giving incorrect results. For the cone case, the method that was successful for wedge flow became inadequate after computing large distances from the tip, and a third method was used to handle this situation.

It was necessary to compute over such large regions because of the behavior of the pressure on the cone surface. On the wedge, for all cases computed, the pressure monotonically approached the value computed for equilibrium wedge flow. This was shown to be the proper value. On the cone, for the cases computed thus far at least, the pressure goes below the value for equilibrium conical flow but then slowly approaches it from below. This is the most striking difference between the wedge and cone flows.

Qualitatively, the cone flow properties behave like those for wedge flow, except for the difference just noted. The starting numerical process had to be different because of the singular nature of the initial, frozen, conical flow. A sketch showing the starting process is given in Fig. 1. The calculation is started from a frozen conical flow characteristic BC, which is computed separately. In wedge flow one can start in the same way, but it is often convenient to have just two initial points, one at the tip and the other on the straight, frozen shock. Although this procedure is also possible for the cone, it leads to prohibitively large errors. The results for shock-wave angle, temperature, etc., are qualitatively the same as in wedge flow. In particular, there is a relaxation layer always present at the shock and an entropy layer near the body even far downstream from the tip. For the cone, however, the thickness of the entropy layer must approach zero sufficiently far downstream of the tip just from continuity considerations.

A reliable check on the computations near the tip was available for the wedge case, in that the shock curvature and flow variable gradients could be computed easily and independently.[5] Alternatively, these can be used as an aid in starting the computations. As will be discussed later, such information would be even more valuable for the cone case. Here, however, the initial gradients are not easily obtainable because of the singularity at the tip. They could be obtained by a perturbation of frozen conical flow. However, the form of the perturbation is not known a priori; it may not be linear. This matter is being investigated, but no results have been obtained yet.

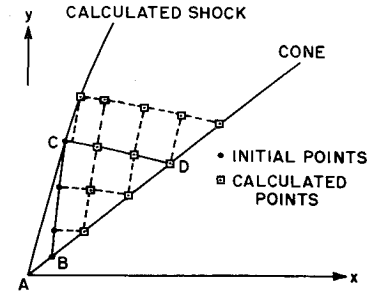

Fig. 1 Starting procedure for calculation of flow over a cone with frozen conical flow in region *ABC*.

2. Characteristic Equations

The steady, inviscid, axisymmetric flow of a pure diatomic gas will be considered; heat conduction and diffusion effects are neglected. It is assumed that the temperatures and pressures are such that the translational and rotational degrees of freedom are in equilibrium, and chemical effects are frozen. Only the vibrational energy departs from its equilibrium value. The departure from equilibrium is governed by the rate equation

$$dE_i/dt = [E_i(T) - E_i]/\tau \tag{2.1}$$

where E_i is the local value of the vibrational energy, $E_i(T)$ is the vibrational energy if equilibrium existed at the local temperature T, τ is the relaxation time, and the derivative is the substantial derivative. For quantized simple harmonic oscillators,

$$E_i(T) = R\Theta_i/[\exp(\Theta_i/T) - 1]$$

where Θ_i is the characteristic vibrational temperature and R is the gas constant per unit mass. The variation of τ with temperature and pressure was approximated by

$$\tau \propto [\exp(C/T)^{1/3}]/p$$

where the constant C was evaluated for various temperature intervals by fitting the data of Blackman,[12] and p is the pressure; reference values of T and p are taken at the tip of the cone surface. With the freestream flow in the x direction and with θ the angle of flow with respect to the x direction, the equations of the characteristics are

$$dy/dx = \tan(\theta \pm \mu) \qquad dy/dx = \tan\theta$$

i.e., the Mach lines based on the frozen Mach angle μ and the streamlines.

As discussed in Ref. 1, using entropy as a dependent variable leads to large errors in the computation because of the behavior of the "vibrational temperature" at the shock wave. The dependent variables chosen were p, θ, E_i, q, and T, where q is the magnitude of the velocity. The compatibility equations are

$$\frac{\sin 2\mu}{2\gamma_a p}\frac{\partial p}{\partial \xi} - \frac{\partial \theta}{\partial \xi} = -\epsilon \sin\mu \tag{2.2}$$

$$\frac{\sin 2\mu}{2\gamma_a p}\frac{\partial p}{\partial \eta} + \frac{\partial \theta}{\partial \eta} = -\epsilon \sin\mu \tag{2.3}$$

$$\frac{\partial E_i}{\partial s} = \frac{E_i(T) - E_i}{\tau q} \tag{2.4}$$

$$\frac{1}{q}\frac{\partial q}{\partial s} = -\frac{\sin^2\mu}{\gamma_a p}\frac{\partial p}{\partial s} \tag{2.5}$$

where

$$\epsilon = \frac{E_i(T) - E_i}{\tau q C_{pa} T} + \frac{\sin\theta}{y}$$

ξ, η, and s are arc lengths along the right and left Mach lines and streamline, respectively, $\gamma_a = 1.4$ is the ratio of frozen specific heats, and C_{pa} is the frozen specific heat. In addition, the energy equation is needed:

$$C_{pa}T + E_i + (q^2/2) = h_t \tag{2.6}$$

where h_t is the constant total enthalpy. For a more complete discussion of these equations, see Ref. 1.

3. Numerical Technique

In calculating nonequilibrium wedge flow, it was found that there were difficulties with the standard method, and a more accurate technique was developed. This new technique gave acceptable results; however, these results always showed some oscillations in the pressure on the wedge surface. These oscillations decreased with decreasing grid size but were also dependent on the method of starting the computation. When this method was used for cone flow, the oscillations eventually became so large that the computation could not be continued. A third technique, which involves just a

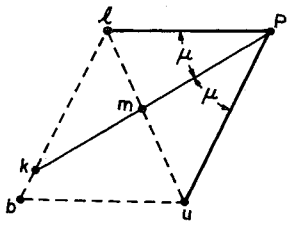

Fig. 2 Grid schemes for the numerical techniques.

slight change of the standard one, finally gave acceptable results.

The standard technique[17] is illustrated in Fig. 2. With all quantities known at points l and u, the defining relations for the Mach lines, together with (2.2) and (2.3), are used to determine x, y, p, and θ at the new point P. With θ known, the intersection of the streamline with the diagonal line lu, point m, is determined. Linear interpolation is used to determine conditions at m, and (2.4) and (2.5) give q and E_i at P. This process is iterated and would be correct to second order in grid size except for the linear interpolation.

The second technique makes use of the additional point b and series expansions about the midpoint of the characteristic net after transforming to characteristic variables. It is correct to second order without iteration, and there are no interpolations. More details of this method are found in Ref. 1.

The third technique is basically the same as the standard one except that the streamline is carried back to point k, its intersection with the characteristic bl (or bu). Again linear interpolation is used to determine conditions at k, and the process is iterated. Previously, it was felt that the difficulties with the standard method were caused by linear interpolation, but this is not the case, since the third method does not exhibit these.

Results for the case of wedge flow are shown in Fig. 3, where the three techniques just described are labeled two-point iterative, three-point noniterative, and three-point iterative. In dimensionless form, pressure is plotted vs distance along the wedge. These results show two features of the standard method. First, it gives pressures that are always below the other two methods, and second, there is a drastic effect when the grid size is increased. (The effects on T and E_i are negligible.) The vertical bars indicate positions where the grid size was increased by a factor of two. The three-point noniterative case is also affected. If the calculation is carried out further, the oscillations tend to grow. The effect on the three-point iterative case is negligible. Actually, the wedge case can be carried out without increasing the grid size, but in the cone case several such increases are necessary. The results shown for the wedge case are representative of what occurs for the cone, except

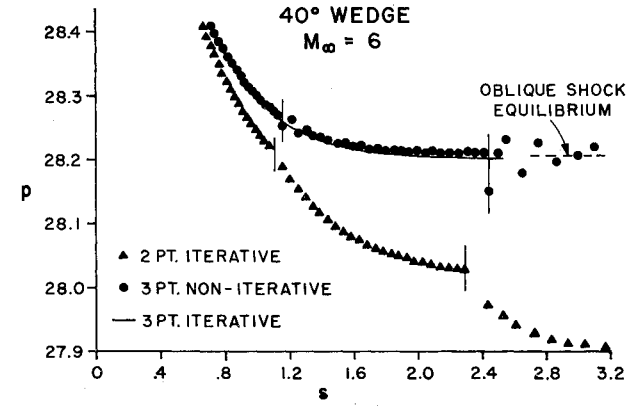

Fig. 3 Dimensionless pressure vs distance along the wedge surface computed by three numerical techniques. The grid size was doubled at positions indicated by vertical bars.

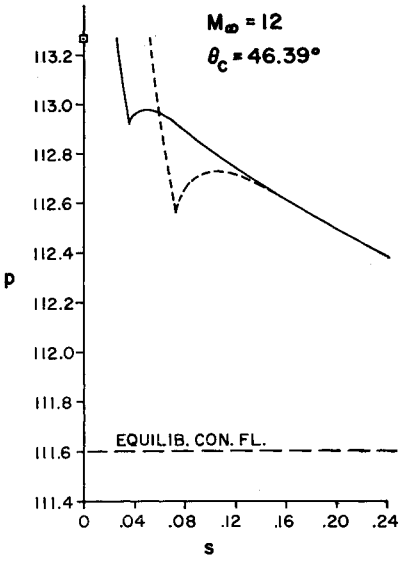

Fig. 4 Dimensionless pressure vs distance along the cone surface for two positions of the initial characteristic; ⊡ indicates pressure for frozen conical flow.

that, for the rising portion of the pressure (to be described in the next section), the three-point iterative technique does show some effect due to increasing the grid size.

The authors do not have an explanation for the differences caused by the slight change from the two-point iterative to the three-point iterative methods. Intuitively, it seems better to make use of information at the third point, but the explanation must lie in the way in which errors are propagated, since the methods give essentially the same results initially.

The initial results for pressure on the cone surface are shown in Fig. 4 in dimensionless form. Results for two positions of the starting characteristic, BC of Fig. 1, are shown. All three methods gave essentially the same results in this region. The steep gradient occurs along the portion BD of the cone surface. The rapid change in the tip region requires rather small grid sizes, and this makes the computations tedious. An analytic solution valid in the tip region would be very helpful.

4. Results

Some representative results will be given for the flow of N_2 over a cone. The freestream temperature is taken as 300°K. Actually, only Θ_i/T_∞ and C/T_∞ need to be specified for a fixed freestream Mach number. For N_2, Θ_i = 3336°K was used. The freestream pressure does not have to be specified except to obtain $\tau_0 q_\infty$, where τ_0 is the relaxation time evaluated on the body at the tip; this length was used

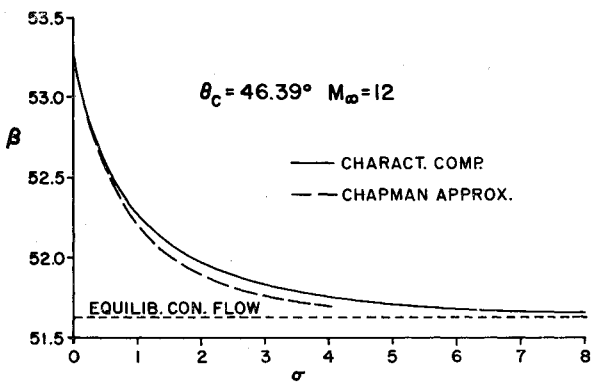

Fig. 5 Shock wave angle vs dimensionless arc length along shock.

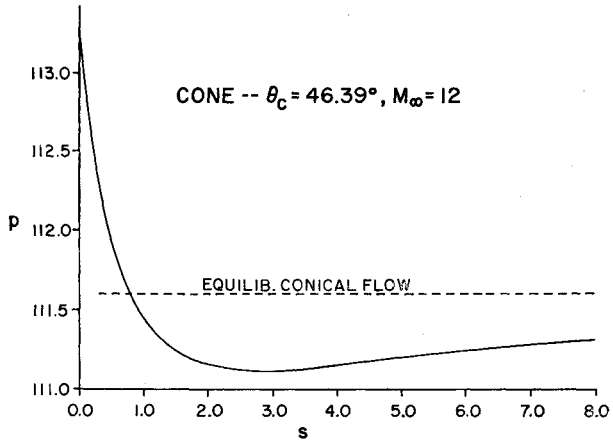

Fig. 6 Dimensionless pressure vs distance along the cone surface.

to nondimensionalize all distances. The quantities p, T, and q were made dimensionless by their freestream values, E_i by $C_{pa}T_\infty$. Results for a freestream Mach number $M_\infty = 12$ and cone angle $\theta_c = 46.39°$ will be given. For this case $\tau_0 q_\infty = 0.015$ cm if $p_\infty = 1$ atm; for other freestream pressures this length is divided by p_∞ in atmospheres.

In Fig. 5 the shock wave angle β is plotted as a function of arc length along the shock and shows a monotonic decrease from the frozen value to the equilibrium value for conical flow. This latter value is taken from Ref. 13. In Fig. 6 the pressure on the cone surface is shown going below the value for equilibrium conical flow and then slowly approaching this value from below. In the region shown, the error in p is at most 0.01. The calculations have been extended to $s = 20$, where the error, due to oscillations and increase of grid size, grows to about 0.05; at $s = 20$, p has reached 111.5. This overexpansion is the most striking difference between the cases of wedge and cone flow. In all cases computed so far (ranging from $M = 6$, $\theta_c = 48°$ to $M_\infty = 15$, $\theta_c = 15°$), the overexpansion occurs for cones but not for wedges. The authors do not know if this behavior is always to be expected; from physical principles this correlation is neither necessary nor prohibited. In Fig. 7a the temperature distribution along the cone surface is shown. The equilibrium value attained is higher than that for equilibrium conical flow. The same situation occurs for wedge flow. In Fig. 7b the distribution of E_i along the cone surface is shown. Using as a criterion for equilibrium $[E_i(T) - E_i]/E_i(T) = 0.01$, equilibrium is reached at $s = 5$. The region in which equilibrium is attained is shown in Fig. 8.

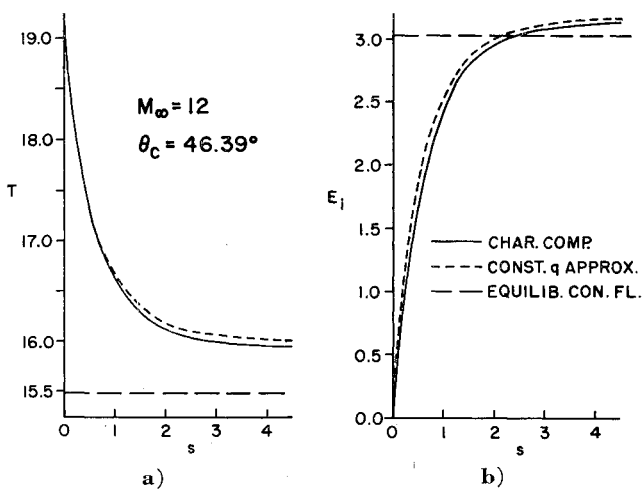

Fig. 7 a) Dimensionless temperature and b) vibrational energy vs distance along the cone surface.

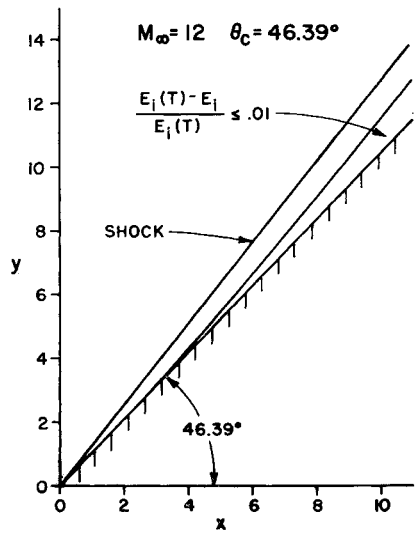

Fig. 8 Region in which equilibrium has been attained.

Just as for the case of wedge flow, there will be a relaxation layer near the shock.

In Ref. 1 it was shown that, in addition, there will be an entropy layer at the wedge surface. This also occurs for cone flow. In Fig. 9 the distributions of p and T are shown at two positions across the shock layer normal to the cone surface; the same quantities are also shown for equilibrium conical flow. For the equilibrium region, the highest temperature occurs on the cone surface. The resulting entropy distribution is shown in Fig. 10, normalized with the cone and shock values. Thus, far from the tip the flow can be divided into three regions: the entropy layer at the cone surface, the equilibrium conical flow, and the relaxation layer at the shock. The situation is the same for wedge flow, but for cone flow the thickness of the entropy layer must vanish at large s, just from conservation of mass and the fact that in equilibrium the entropy is constant along streamlines. To maintain the accuracy of the computations, the grid size near the cone surface would have to be governed by the thickness of this layer, whereas throughout most of the flow the grid size should be larger. This would present difficulties

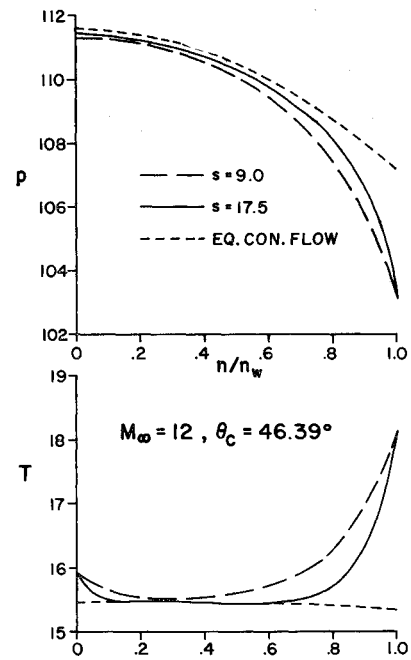

Fig. 9 Dimensionless pressure and temperature vs distance normal to the cone surface.

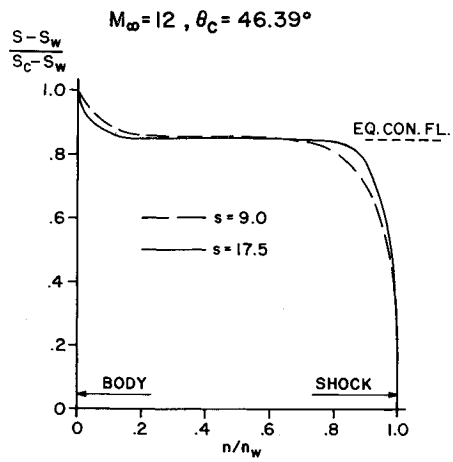

Fig. 10 Relative change of entropy vs distance normal to the cone surface.

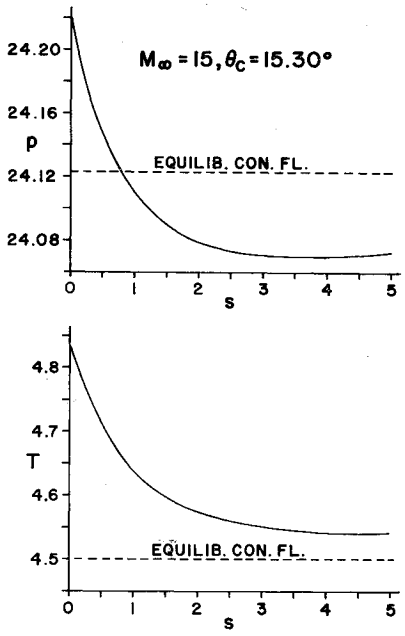

Fig. 11 Dimensionless pressure and temperature vs distance along cone surface.

and indicates that perhaps another method should be used, e.g., one that follows streamlines.

The pressure and temperature distributions along the cone surface are shown in Fig. 11 for $M_\infty = 15$ and a cone angle of 15.30°.

5. Discussion

One of the main uses of the numerical solutions described in the foregoing is to test approximate solutions. An approximate solution for T and E_i along the cone surface can be obtained easily if the velocity q is assumed constant. Then (2.4) and (2.6) can be integrated numerically. The results of such an approximation are shown in Figs. 7a and 7b, and the agreement with the characteristic computation is quite good. This approximation is the analog of that given by Bloom and Steiger[7] for the flow along the surface beyond the sonic point of a blunt body.

An approximate method of obtaining the shock shape for nonequilibrium flow over a cone was developed by Chapman (see Ref. 14). There are three main assumptions in this method: 1) the flow variables differ by only a small amount from a reference flow, e.g., frozen or equilibrium flow; 2) this reference flow is constant; and 3) the difference between the shock and cone angles is small compared to the cone angle. Also, the rate equation is written in terms of enthalpy, and the relaxation time is assumed constant. In polar coordinates (r,ϕ), the expression for the shock shape is

$$\phi - \phi_e = 2(\phi_f - \phi_e)(\lambda - 1 + e^{-\lambda})/\lambda^2$$

$$\lambda = r/\tau_0 q_0$$

where the subscripts f, e, and 0 refer to frozen and equilibrium shock angles and the frozen reference conical flow. Transforming this to β vs σ gives the result shown in Fig. 5. The agreement with the characteristic computation is quite good.

References

[1] Sedney, R., South, J. C., and Gerber, N., "Characteristic calculation of non-equilibrium flows," Aberdeen Proving Ground, BRL R-1173 (April 1962); also *Proceedings of the AGARD Meeting on High Temperature Effects on Hypersonic Flow* (Pergamon Press, Oxford, 1962).

[2] Lick, W., "Inviscid flow of a reacting mixture of gases around a blunt body," J. Fluid Mech. **7**, 128–144 (1960).

[3] Hall, J. G., Eschenroeder, A. Q., and Marrone, P. V., "Blunt-nosed inviscid air flows with coupled nonequilibrium processes," J. Aerospace Sci. **29**, 1038–1051 (1962).

[4] Li, T. Y., "Recent advances in nonequilibrium dissociating gasdynamics," ARS J. **31**, 170–178 (1961).

[5] Sedney, R., "Some aspects of nonequilibrium flows," J. Aerospace Sci. **28**, 189–197 (1961).

[6] Napolitano, L. G., "Non-equilibrium centered rarefaction for a reacting mixture," Arnold Eng. Dev. Center AEDC-TN-60-129 (1960).

[7] Bloom, M. H. and Steiger, M. H., "Inviscid flow with nonequilibrium molecular dissociation for pressure distributions encountered in hypersonic flight," J. Aerospace Sci. **27**, 821 (1960).

[8] Lin, S. C. and Teare, J. D., "A streamtube approximation for calculation of reaction rates in the inviscid flow field of hypersonic objects," Avco-Everett Research Lab., Res. Note 223 (1961).

[9] South, J. C., "Application of Dorodnitsyn's integral method to non-equilibrium flows over pointed bodies," NASA TND-1942 (August 1963).

[10] Cleaver, J. W., "The two-dimensional flow of an ideal dissociating gas," College Aeronaut., Cranfield, Rept. 123 (1959).

[11] Capiaux, R. and Washington, M., "Non-equilibrium flow past a wedge," IAS Preprint 62-99 (1962).

[12] Blackman, V., "Vibrational relaxation in oxygen and nitrogen," J. Fluid Mech. **1**, 61 (1956).

[13] Kelly, P. D., "Conical flow parameters for air and nitrogen in vibrational equilibrium," Aberdeen Proving Ground, BRL R-1164 (March 1962).

[14] Stephenson, J. D., "A technique for determining relaxation times by free-flight tests of low-fineness-ratio cones; with experimental results for air at equilibrium temperatures up to 3440°K," NASA TN D-327 (1960).

[15] Lee, R. S., "A unified analysis of supersonic nonequilibrium flow over a wedge," IAS Paper 63-40 (January 1963).

[16] Capiaux, R. and Washington, M., "Nonequilibrium flow past a wedge," AIAA J. **1**, 650–660 (1963).

[17] Isenberg, J. S., "The method of characteristics in compressible flow—Part I," Rept. F-TR-1173A-ND(GDAM A9-MII/1), Wright Field, Dayton, Ohio (1947).